

A pH-Controllable Imprinted Composite Membrane for Selective Separation of Podophyllotoxin and Its Analog

Huiling Cheng, Xiufang Zhu, Shunxiang Yang, Yuxi Wu, Qiue Cao, Zhongtao Ding

Key Laboratory of Medicinal Chemistry for Nature Resource, Ministry of Education; School of Chemical Science and Technology, Yunnan University, Kunming, Yunnan 650091, People's Republic of China

Correspondence to: Z. Ding (E-mail: ztding@ynu.edu.cn)

ABSTRACT: A molecularly imprinted composite membrane (MICM) with pH-controllability and selectivity to podophyllotoxin (PPT) was prepared using a polyvinylidene fluoride (PVDF) microfiltration membrane as the support. The functional monomer is 1-phenyl-3-methyl-4-methacryloyl-5-pyrazolone (PMMP), which is a new β -diketone compound with enol/ketol tautomerization. In this study, imprinting parameters, including the amounts of functional monomer and cross-linker, and immersion time of membrane in the imprinting solution, were optimized by equilibrium adsorption experiments. Pore structure and surface morphology of the optimal MICM (MICM₂) was characterized. Finally, competitive permeability of PPT in the presence of its analog 4'-demethylpodophyllotoxin (DMEP) was measured under the drive of concentration difference. The results reveal that the surface morphology and pore structure of MICM₂ are structurally different from those of the control nonimprinted membrane. As a result, MICM₂ could efficiently recognize PPT in a complex system due to a better structural matching and the interaction between the functional groups of MICM₂ and PPT. However, the most interesting finding is its pH-controllability. The membrane could switch the preference to either PPT or DMEP with the change of pH values in the sample solution. At pH values smaller than 8.4, it led to a faster transportation of PPT, while the situation reversed to DMEP at pH values greater than 8.4. This peculiar property would lead this imprinted membrane to have potential application in the separation and enrichment of PPT, and the new functional monomer PMMP exhibited an attractive application prospect in the functional material fields. © 2012 Wiley Periodicals, Inc. *J. Appl. Polym. Sci.* 000: 000–000, 2012

KEYWORDS: molecularly imprinted composite membrane; pH-controllability; β -diketone monomer; podophyllotoxin

Received 23 March 2012; accepted 4 June 2012; published online

DOI: 10.1002/app.38144

INTRODUCTION

The plant species *Sinophyllum emodi* has been used as a traditional medicine herb in Chinese folk remedies for about 1000 years. Numerous studies have revealed that podophyllotoxin (PPT) extracted from *S. emodi* is the key ingredient contributing to its remarkable antiviral and anticancer activities.¹ Moreover, PPT is an important lead compound for some anticancer therapeutic agents, such as Etoposide (VP16) and Teniposide (VM-26).² In recent years, the increasing demands have led the preparation of PPT to become a hot spot of research. However, completely chemical synthesis of the PPT skeleton, up to now, is not a practical option from a commercial point of view. Extraction from plants is still the main source of PPT. The extracting process is always tedious and inefficient due to the poor affinity and selectivity of conventional separation materials. Therefore, it is crucial to develop an effective separation material with high affinity and selectivity to PPT.

Membrane is an interphase between two adjacent phases, acting as a selective barrier and regulating the exchange of substances between the two compartments. Compared with other unit operations, membrane processes can be performed isothermally at low energy consumption. Also, membrane processes are easy to be upscaled or downscaled as well as integrated into other separations or reactions. Therefore, membranes are widely used in various separating processes including the separation of biomaterials, catalysis, and lab-on-chip technologies.³ However, general membranes suffer from the lack of selectivity for the constituents with similar molecular weights and volumes, which greatly limits its application in many fields.

The surface functionalization of commercial membranes has already become a key technology in membrane modification.⁴ By covering tailored functional polymer layers on the pore walls of membrane, it is possible to increase the membrane's selectivity or permeability, or to introduce other desired properties.⁵

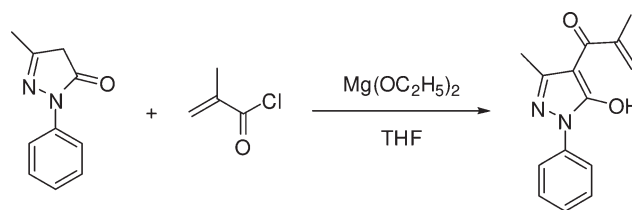
Molecular imprinting is regarded as the most efficient way to introduce molecular recognition sites into polymeric materials. Introduction of imprinting technology into membrane modification would produce 'tailored' barrier in the membrane.⁶ Among all molecularly imprinting composite membranes (MICMs), stimuli-responsive membrane is the most fascinating material. By grafting pH-responsive or temperature-responsive polymers in a porous base membrane, it is possible to switch its permeability.⁷ But current intelligent materials are almost confined to polyacrylic acid, polymethacrylic acid or poly *N*-isopropylacrylamide.^{8,9} Acyl pyrazolones are heterocyclic β -diketone reagents. Their enol/keto tautomerization in response to the change of polarity or pH value in solvents has aroused increasing interests of scientists and been used in functional material fields.¹⁰ However, the application of acyl pyrazolones in molecular imprinting technique has never been published up to now. It would be an interesting study to explore a novel stimuli-responsive intelligent membrane with a predetermined affinity to PPT using an acyl pyrazolone compound as the functional monomer.

As a part of our systematic studies,¹¹ this study aims to synthesize a new pH-responsive functional monomer, namely, 1-phenyl-3-methyl-4-methacryloyl-5-pyrazolone (PMMP). Its stimuli-responsibility was validated by UV spectroscopy analysis in solvents at various pH values. On the support of a commercial polyvinylidene fluoride (PVDF) microfiltration membrane, the copolymerization of PMMP with the excess cross-linker, i.e., ethylene glycol dimethacrylate (EDMA), was initiated in the presence of PPT. Imprinting parameters, including the amounts of functional monomer and cross-linker, and immersion time of membrane in the imprinting solution, were optimized according to the specific equilibrated binding amounts to PPT. The optimized MICM was characterized and evaluated based on the results of scanning electron microscope (SEM), nitrogen sorption analysis, and ultra performance liquid chromatography (UPLC). Finally, the optimized MICM was successfully used to competitively transport PPT in a complex system and showed a pH-controllable effect. To the best of our knowledge, this is the first report of molecularly imprinted membrane for PPT.

EXPERIMENTAL

Reagents and Materials

PPT and 4'-demethylpodophyllotoxin (DMEP) were purchased from Langze Pharmaceutical Technology (Nanjing, China). *S. emodi* was bought from Juhucun Chinese Herbal Medicine Market (Kunming, China). PVDF microfiltration membrane, with nominal pore size of 0.45 μm and thickness of 125 μm , was obtained from Yadong Heji Rosin (Shanghai, China). Ethylene glycol dimethacrylate (EDMA) was purchased from Suzhou Anli Chemical Plant (Jiangsu, China) and distilled to remove the stabilizer before use. Azobisisobutyronitrile (AIBN) was obtained from The Fourth Reagent Plant of Shanghai (Tianjing, China) and recrystallized in ethanol. Dichloromethane was distilled over calcium hydride. Tetrahydrofuran (THF) was distilled over sodium and benzophenone. Other chemicals were of analytical grade.



Scheme 1. Synthesis of PMMP.

Instrumental

An ultra performance liquid chromatography system (UPLC) (Waters) was used in the chromatographic evaluation. The analytical column was a Waters Acquity UPLC BEH C_{18} column (100 \times 2.1 mm² i.d.; 1.7 μm). The flow rate was kept at 0.2 mL/min. The mobile phase was composed of A (CH_3OH) and B (H_2O). The linear gradient elution was programmed as follows: 35–70% B, 0–6 min; 70–100% B, 6–14 min; 100% B, 14–25 min. The detection wavelength was 211 nm. The column was maintained at 30°C. Under the above conditions, PPT and DMEP could be isolated from other interfering components with the calibration equation of $A = 26119C - 6284.5$ ($R = 0.9992$, $R.S.D = 1.21\%$) for PPT in the concentration range of 2–100 $\mu\text{g/mL}$, and $A = 29336C - 23316$ ($R = 0.9983$, $R.S.D = 1.35\%$) for DMEP in the range of 1.082–50.40 $\mu\text{g/mL}$, where A and C are the peak area and concentration of a substrate, respectively.

A Shimadzu UV-2401 spectrophotometer (Tokyo, Japan) was used to determine the UV spectra of PPT. A HZ constant temperature bath oscillator (Jiangsu, China) was utilized in the binding experiments. An Avance 300 NMR (Bruker, Switzerland) was used to elucidate the structure of the new functional monomer PMMP. Mass spectra were measured in a system consisting of an Agilent 1100 chromatograph coupled to a time-of-flight mass detector (LC/MSD TOF 1969), operating in the positive ion mode of electrospray ionization (ESI) source. IR spectra (4000–400 cm^{-1}) were recorded on Fourier transform infrared (FTIR) (Avatar 360, Nicolet Company) by KBr pellet method.

Synthesis of Novel Monomer

The preparation process of 1-phenyl-3-methyl-4-methacryloyl-5-pyrazolone (PMMP) was shown in Scheme 1. Magnesium ethoxide (0.01 mol) was added to a solution of 1-phenyl-3-methyl-5-pyrazolone (0.01 mol) in dry THF (50 mL). The mixture was magnetically stirred and refluxed for 4 h. Then, a solution of methacryloyl chloride (0.01 mol) in THF (25 mL) was added dropwise in an ice bath. After stirred at room temperature for more 4 h, the solution was poured into 10% HCl (200 mL) and extracted with CHCl_3 (2 \times 50 mL). The combined organic layers were washed with water (2 \times 50 mL) and dried with anhydrous magnesium sulfate. After removing the solvent, the residue was purified by column chromatography on silica gel (200–300 mesh, eluted with petroleum ether/ethyl acetate) to afford PMMP (1.58 g, 90.80%), which is in the form of solid with a pale yellow color.

¹H-NMR (300 MHz, CDCl_3), δ : 10.55 (brs, 1H), 7.84 (d, $J = 8.1$ Hz, 2H), 7.44 (t, $J = 8.1$ Hz, 2H), 7.27 (t, $J = 8.1$ Hz, 1H),

Table I. Imprinting Conditions of Various Protocols

Membrane	PPT (mmol)	PMMP (mmol)	EDMA (mmol)	Soaking-time (s)	PPT/PMMP/EDMA (molar ratio)
MICM ₁	1	2	20	180	1:2:20
MICM ₂	1	4	20	180	1:4:20
MICM ₃	1	6	20	180	1:6:20
MICM ₄	1	8	20	180	1:8:20
MICM ₅	1	4	10	180	1:4:10
MICM ₆	1	4	30	180	1:4:30
MICM ₇	1	4	40	180	1:4:40
MICM ₈	1	4	50	180	1:4:50
MICM ₉	1	4	20	30	1:4:20
MICM ₁₀	1	4	20	1800	1:4:20
MICM ₁₁	1	4	20	3600	1:4:20

5.60 (brs, 1H), 5.47 (brs, 1H), 2.34 (s,3H), 2.07 (s, 3H); ¹³C-NMR (75 MHz, CDCl₃) δ: 193.6 (s), 161.8 (s), 147.9 (s), 142.6 (s), 137.3 (s), 129.1 (d, 2C), 126.6 (d), 121.2 (t), 120.7 (d, 2C), 102.5 (s), 18.7 (q), 15.8 (q). ESI-MSD/TOF: 243.1128 ([M+H]⁺, 243.1128).

Preparation of MICMs

A series of imprinted membranes, labeled as MICM₁, MICM₂,..... MICM₁₁, were prepared with various amounts of functional monomer and cross-linker, and immersion time durations in prepolymerization solution according to Table I. The required amounts of functional monomer (PMMP), template molecule (PPT), cross-linker EDMA and initiator AIBN (10 mg) were dissolved in 10 mL of CHCl₃. The mixture was ultrasonically outgassed for 5 min. Then, a circular PVDF membrane (area 2.25 cm²) was immersed in this solution. After a required time, the membrane was taken out and clapped between two glass plates, sealed and heated at 60°C for 24 h. After completing the polymerization, the membrane was placed in a Soxhlet apparatus and washed with methanol/acetic acid (9:1, v/v) until no PPT in the eluent could be detected at 292 nm by UV method. The membrane was then rinsed with methanol to remove residual acetic acid and dried under vacuum.

As a control, the nonimprinted blank membranes (NICM₁₋₁₁) were also prepared simultaneously in the absence of the template (PPT) and treated with the same procedure.

Equilibrium Binding Experiments

Each of the imprinted membranes and control nonimprinted membranes (20.0 mg of each) was placed in a 25-mL Erlen-Meyer flask and mixed with 10 mL of PPT methanol solution (2.4 mmol/L), respectively. The mixtures were oscillated at room temperature for 6 h. The concentration of free substrate in the solution was determined by UPLC. The adsorption capacity (Q), which is defined as the molar concentration (μmol) of the substrate binding to 1 g of polymer membrane, was calculated by subtracting the concentration of free substrate from the initial concentration. The average values of triplicate independent results were obtained.

Characterization of Membranes

The surface morphology of membrane was observed using a Hitachi S-520 field emission scanning electron microscope (Tokyo, Japan). Before scanning with a SEM, each membrane sample was quenched by liquid nitrogen and coated with a layer of gold.

The pore diameter of membrane was determined by nitrogen adsorption. The adsorption/desorption analysis was done using a NOVA 2000e gas sorption analyzer (Quantachrome). Before the observation, the sample was outgassed at 100°C for about 1 h.

Permeation Experiment

Selective transportation of substrates was measured using an H-Shape permeation device with two compartment cells, each with a volume of 70 mL. The membrane was fitted tightly at the connecting joint between the two cells. The area available for diffusion was about 1.13 cm². Sixty milliliter of PPT/DMEP mixture (200 μg/mL, each, in CH₃OH) or real herb sample (the preparation method as described in previous literature³) was added into the left cell. The right cell was filled with the same amount of solvent. Each cell was stirred by a mechanical stirrer at a constant speed. The substrate penetrating through the membrane from the right cell was investigated by the removal of sample solution (200 μL) from the right cell with an interval of 1 h in the range of 0–12 h. The concentration of substrate was analyzed by UPLC based on the established calibration curves. The penetration amount was defined as the mass of PPT (μg) per membrane barrier (cm²). After each sampling, 200 μL of fresh solvent was added to maintain the same volume of solution (60 mL) in the right cell.

RESULTS AND DISCUSSION

Synthesis of New Monomer and its Spectral Property

Synthesis of New β-Diketone Monomer. Being a type of β-diketone compounds, most acyl pyrazolones could be tautomerized between ketone and enol forms with the change of pH value or the polarity of solvents. To achieve a stimuli-responsive MICM possessing PPT selectivity, a new heterocyclic compound 1-phenyl-3-methyl-4-methacryloyl-5-pyrazolone (PMMP) was synthesized using 1-phenyl-3-methyl-5-pyrazolone (PMP) and methacrylate chloride (MC). Its structure was elucidated by NMR and MS data, and its stimuli-responsibility was characterized by UV spectroscopy.

Stimuli-Responsibility. Figure 1 shows the UV spectra of 0.10 mmol/L PMMP in four different solvents, including CH₃OH, CH₃CN, CHCl₃, and Et₂O. The polarity parameters of them were 6.6, 6.2, 4.4, and 2.2, respectively. It can be seen that PMMP exhibits two absorption peaks in the solvents with moderate polarity (CH₃CN and CH₃OH). The first peak at 210 nm can be attributed to the E band of benzene ring and the second one at 250 nm might be the coordination effect of the B band of benzene and pyrazolone matrix.¹² When the solvent was replaced with weakly polarized ones (CHCl₃ and Et₂O), the absorbance at 210 nm reduced remarkably. As shown in Figure 1, the first peak of PMMP in CHCl₃ decreased about 50% comparing with those in CH₃CN and CH₃OH, and that in Et₂O

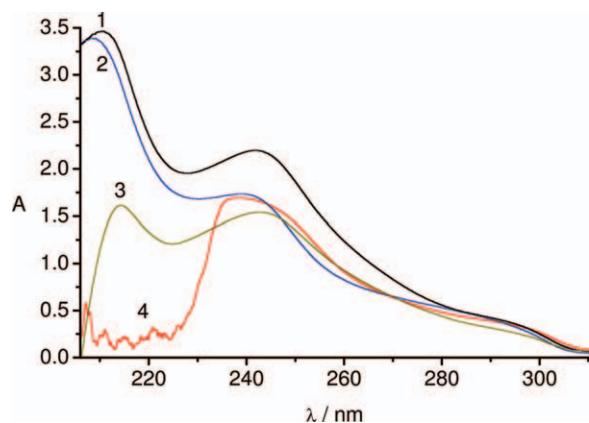


Figure 1. UV spectra of 0.10 mmolL^{-1} PMMP in different solvents. 1- CH_3CN ; 2- CH_3OH ; 3- CHCl_3 ; and 4- Et_2O . [Color figure can be viewed in the online issue, which is available at wileyonlinelibrary.com.]

disappeared completely. Figure 2 shows the UV spectra of PMMP in CH_3OH with different pH values (3.6, 7.6, and 10.1). It can be seen that with the increase of pH values, the second peak exhibits a red shift due to the change in the structure of pyrazolone matrix at various pH values.¹³ These results reveal that PMMP certainly possesses stimuli-responsibility.

Prediction of the Binding by UV Spectrophotometry. The recognition ability of the imprinted composite membrane to template molecule results from prepolymerized host-guest structure preservation in a functional polymer matrix.¹⁴ Therefore, it is important to investigate the interaction between the template and functional monomer. The interaction between PPT and PMMP was investigated using UV spectroscopy. Here, CHCl_3 was chosen as the solvent because it does not interfere with hydrogen bonding.

As shown in Figure 3, the absorbance of the system decreases gradually with the increase of PMMP amount in the solutions. When the PMMP concentration increases, the first absorption peak of PPT (at 244 nm) exhibits an obvious red shift and a noticeable decreased absorbance. As the molar ratio of PMMP

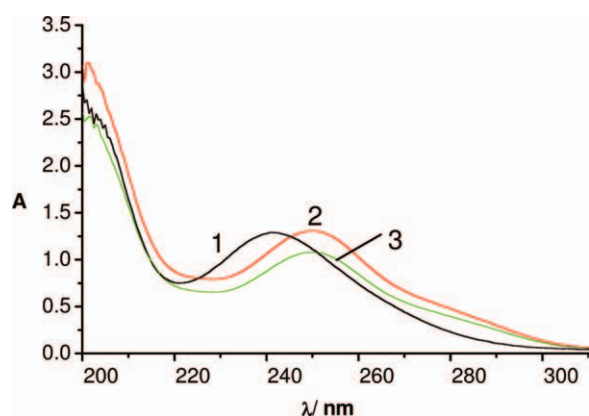


Figure 2. UV spectra of 0.10 mmolL^{-1} PMMP in CH_3OH with different pH values. 1-pH 3.6; 2-pH 7.6; 3-pH 10.1. [Color figure can be viewed in the online issue, which is available at wileyonlinelibrary.com.]

to PPT rises to 5:1, the absorbance at 244 nm approaches to zero and the maximum absorption wavelength (λ_{max}) shifts to 256 nm. The second peak (at 292 nm) shows a blue shift along with reduced absorbance. These obvious changes indicate that a stable complex was formed between PPT and PMMP.¹⁵ As a result, PMMP synthesized in this study can be a suitable functional monomer for PPT and a stimuli-responsive imprinted membrane could be expected.

Optimization of MICM

The copolymerization of the functional monomer PMMP and the cross-linker EDMA, in the presence of the template PPT, occurs on the external surfaces and in the pores of the supporting membrane. In essence, PVDF membrane was only used as the support for functional polymer, while the intelligent polymer coating on the base membrane is the main recognition component of MICM. Therefore, the structural optimization of polymer is vital for the selectivity of MICM.¹⁶

Amounts of Functional Monomer. Four pairs of molecularly imprinted composite membranes (MICM_{1-4}) and control non-imprinted composite membranes (NICM_{1-4}) were prepared with different amounts of functional monomer PMMP (2.0, 4.0, 6.0, and 8.0 mmol). Their equilibrium binding amounts (Q) to PPT were measured in CH_3OH other than CH_3Cl because CH_3OH is extensively used in reverse phase chromatography. The result showed in Figure 4 indicates that the adsorption capacity of MICM increases with the addition of functional monomer PMMP, suggesting that a higher content of PMMP would benefit the formation of PPT-PMMP supermolecular complex. But as reported in the literature,¹⁷ excess functional monomer brought about more nonspecific binding sites. By comparison, MICM_2 prepared with 4 mmol PMMP exhibited the best specific recognition ability with an imprinting factor ($Q_{\text{MICM}}/Q_{\text{NICM}}$) of 1.76. Therefore, the amount of PMMP was fixed at 4.0 mmol in the following investigations.

Amounts of Cross-Linker. The amount of crosslinking agent plays an important role in regulating pore structure of

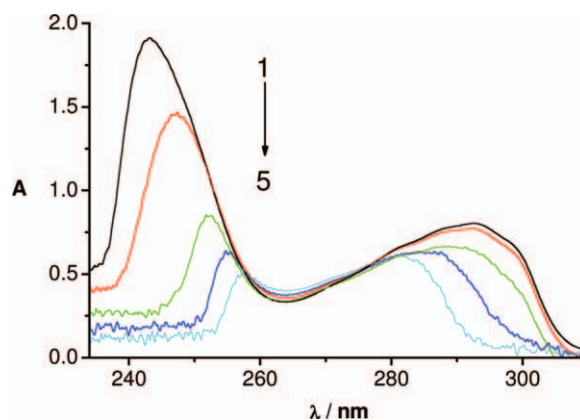


Figure 3. UV spectra of PPT in the presence of PMMP. Concentration of PPT: 0.2 mmolL^{-1} , concentrations of PMMP for curves 1-5: 0, 0.2, 0.6, 1.0, and 1.4 mmolL^{-1} . Correspondingly, pure PMMP solutions were used as blanks. [Color figure can be viewed in the online issue, which is available at wileyonlinelibrary.com.]

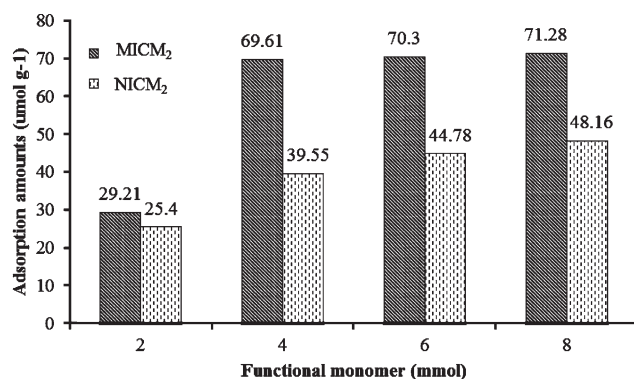


Figure 4. Adsorption amounts of various membranes prepared with different amounts of functional monomer. $M_{\text{membrane}} = 20.0$ mg, $V = 10$ mL, 25°C , adsorption time 6 h.

polymers.¹⁸ Less amount of cross-linker may give rise to less recognition sites in MICM, while too much cross-linker could lead to nonspecific binding sites and a decrease in mass transfer rate. Figure 5 shows the adsorption amounts of PPT on five pairs of imprinted membranes (MICM_{5-8, 2}) and control non-imprinted membranes (NICM_{5-8, 2}) prepared with different crosslinking degrees. It can be seen that the most significant difference in adsorption amounts between MICMs and control NICMs appeared when 20 mmol of cross-linker was used, implying that the MICM prepared with a molar ratio of PPT/PMMP/EDMA of 1:4:20 could lead to the best specific adsorption in the test range.

Soaking-Time of the Support Membrane. In the preparation of MICM, the support membrane was dipped into the imprinting solution, where polymerization coating occurred not only on the external surfaces but also in the internal pores of supporting membranes. Since the diffusion of reaction solution into the inner pores is relevant to immersion time, soaking-time of membrane would influence the thickness of coating layer, morphology and recognition property of the resulting MICM.¹⁹ As can be seen in Figure 6, the imprinted membrane exhibited the best affinity and specific recognition to PPT when the base membrane was immersed for 180 s.

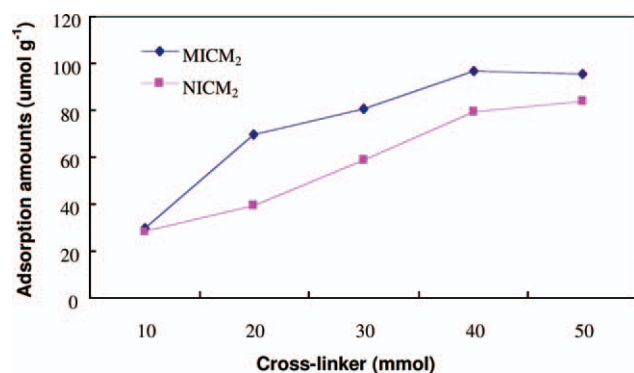


Figure 5. Adsorption amounts of various membranes prepared with different amounts of cross-linker. $M_{\text{membrane}} = 20.0$ mg, $V = 10$ mL, 25°C , adsorption time 6 h. [Color figure can be viewed in the online issue, which is available at wileyonlinelibrary.com.]

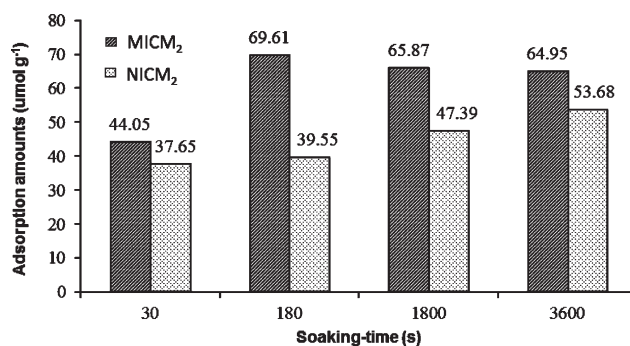


Figure 6. Effect of soaking-time on the adsorption amounts of PPT. $M_{\text{membrane}} = 20.0$ mg, $V = 10$ mL, 25°C , adsorption time 6 h.

Based on the results described above, the optimal conditions for the preparation of PPT imprinting membrane were as follows: the molar ratio of PPT/PMMP/EDMA of 1:4:20, and the soaking-time of PVDF membrane of 180 s. MICM₂ prepared under such conditions gave rise to a higher adsorption amount to PPT ($Q = 69.61$ μmol/g) and a satisfied imprinting factor ($Q_{\text{MICM}_2}/Q_{\text{NICM}_2}$) of 1.76. Therefore, MICM₂ was used for further studies.

Morphology Characterization

SEM Analysis. The surface morphology of the membrane was observed by SEM. As shown in Figure 7, the surface of the untreated PVDF membrane [Figure 7(A)] possesses a symmetric net-like, porous skeleton. The surfaces of NICM₂ [Figure 7(B)] and MICM₂ [Figure 7(C)] are rougher than that of PVDF, suggesting that a thin layer of polymer was coated on PVDF. By comparison, MICM₂ has some large pores scattered on its surface, which could be attributed to the imprinting effect. These imprinting-induced cavities would reduce diffusive resistance and facilitate mass transfer. Therefore, we speculate that a high selectivity and flux could be expected in the case of MICM₂.

Nitrogen Adsorption. The N₂ adsorption/desorption isotherms of MICM₂ and NICM₂ are shown in Figure 8. Both membranes display similar type IV isotherm, which is a character of a mesoporous material.²⁰ However, pronounced differences could be seen in adsorption/desorption isotherms of MICM₂ and NICM₂. The isotherm of MICM₂ shows a hysteresis loop where the desorption curve does not close, instead, level off above the adsorption curve. This is pronounced for the MICM₂ exhibiting no shrinking when subjected to increasing pressure at liquid N₂ temperature.²¹ It implies that those large imprinting pores in MICM₂ have low swelling and solvent uptake rates. On the other hand, the control NICM₂ prepared in the absence of template molecule exhibited overlapped N₂ adsorption/desorption isotherms. So we speculated that the imprinting cavities in MICM₂ played a predominant role in N₂ adsorption/desorption process.

Table II indicates that all parameters including the BET surface area, total pore volume and average pore diameter were slightly higher than those of NICM₂, further suggesting that the template effect existed in the imprinted polymer membrane.

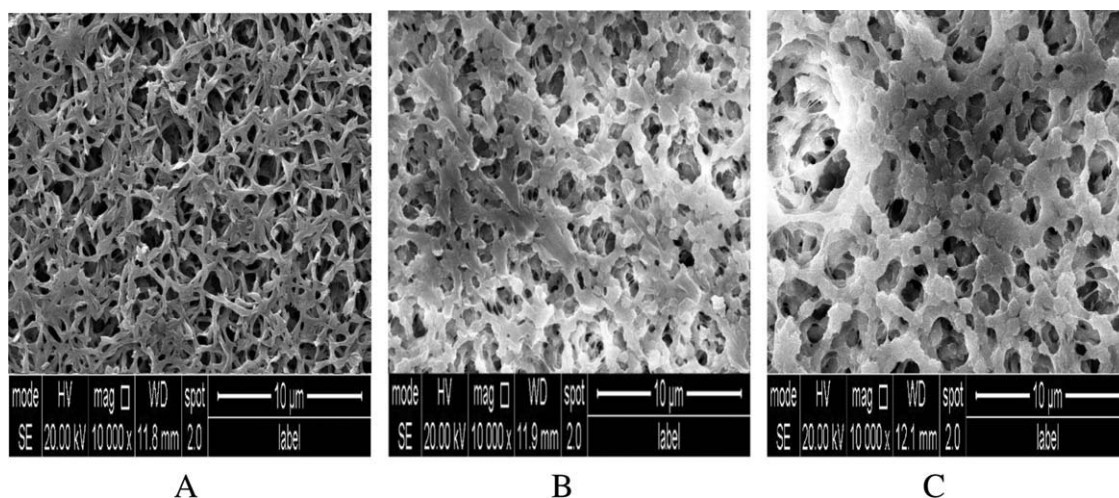


Figure 7. SEM image of PVDF membrane (A), NICM₂ (B), and MICM₂ (C).

IR Spectra. The IR spectra were obtained from PVDF and imprinted composite membrane MICM₂ (Figure 9). The IR spectra of PVDF membrane showed a strong absorption band characterized by CF₂ group at 1185–1280 cm⁻¹. By comparison, the IR spectra of the MICM₂ showed some new peaks at 1740, 1150, and 1300–1000 cm⁻¹, which corresponded to C=O, C—O—C stretching vibration in cross-linker EDMA, and C=N stretching vibration in functional monomer PMMP, indicating successful coating of imprinted polymer on PVDF membrane.

Permeation Selectivity of Membranes

Standard Mixture Analysis. With respect to a membrane process, the overall performance and practical feasibility depend on both selectivity and permeability.²² Demethylpodophyllotoxin (DMEP) is a coexisting interfering compound of PPT in the plant species *S. emodrate*. The separation of PPT from DMEP is a tough task due to their structural similarities.²³ Therefore, DMEP was used as a competitive compound to evaluate the permeating selectivity of MICM₂. Sixty milliliter of PPT/DMEP methanol mixture (200 μg/mL of each) and pure MeOH were

poured into the two cells of H-shape permeation model equipped with MICM₂, NICM₂, or PVDF membrane, respectively. Figure 10 shows the permeating amounts of substrates through various membranes from 0 to 12 h.

As expected, MICM₂ [Figure 10(A)] shows higher selective permeability and transport ability to PPT in the presence of structural analog DMEP compared to NICM₂ [Figure 10(B)]. Taking the penetration amounts at 12 h as a case, MICM₂ (1.13 cm²) can transport 47.33 μg of PPT and 28.10 μg of DMEP, resulting in a satisfied selectivity factor (PPT/DMEP) of up to 1.67, while the corresponding values on NICM₂ were 22.10 μg/cm², 20.08 g/cm² and 1.10. These data demonstrate that MICM₂ has a higher transport rate and selectivity to template than NICM₂, consistent with the results of SEM and N₂ adsorption analyses. The imprinting-induced recognition sites on MICM₂ are complementary with PPT molecule in size, shape and functional group arrangements, and can preferably adsorb PPT from a complex system. According to the “gate effect” mechanism, a facilitated permeation is driven by preferential sorption to template molecule.²⁴ Therefore, PPT can be more efficiently separated from DMEP in the imprinted membrane system of MICM₂.

In the control experiments, the transport ability of the base membrane was also evaluated and the results are shown in Figure 10(C). As expected, PVDF membrane transported nearly equal amounts of PPT and DMEP. These observations demonstrate that the transport selectivity of PPT through MICM₂ is the result of imprinted effect rather than the original property of base membrane.

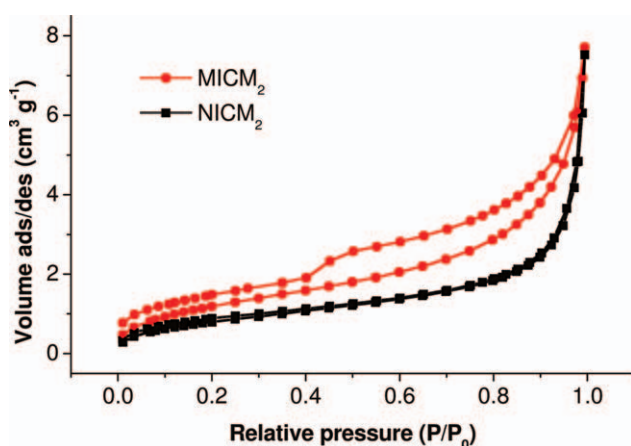


Figure 8. N₂ adsorption/desorption isotherm of MICM₂ and NICM₂. [Color figure can be viewed in the online issue, which is available at wileyonlinelibrary.com.]

Table II. Nitrogen Adsorption Data of MICM₂ and NICM₂

Membrane	Surface area (m ² g ⁻¹)	Pore volume (mL g ⁻¹)	Pore diameter (nm)
MICM ₂	5.17	0.018	14.26
NICM ₂	4.52	0.010	13.19

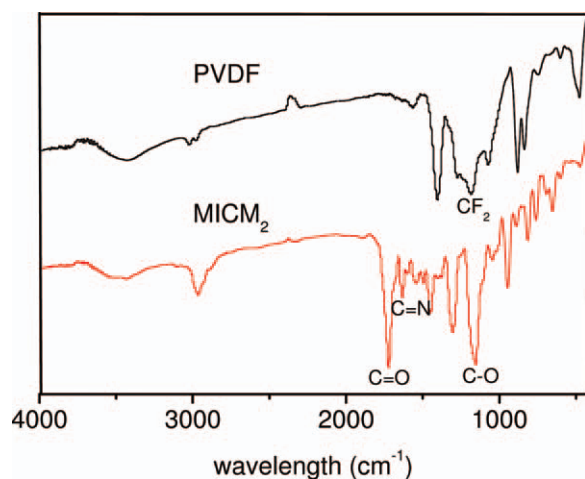


Figure 9. FTIR spectra of a blank PVDF membrane and MICM₂. [Color figure can be viewed in the online issue, which is available at wileyonlinelibrary.com.]

Real Sample Analysis. To explore the application potential of MICM₂ in a real herb solution system, a CH₃OH crude extract of *S. emodrate* (60 mL, 1.0 mg/mL) was used as sample in an H-shape model equipped with MICM₂ or NICM₂. When penetration test had been conducted for 7 h, 200 μ L of diffusion solutions in right cell were taken out and analyzed by UPLC. As a control, the initial sample before penetration was also analyzed. The concentrations of PPT and DMEP in all samples were summarized in Table III. The results show that the mass concentration of PPT is 19.05 times higher than that of DMEP in the initial solution, but the ratio increased to 34.26 times after the treatment of MICM₂ barrier. This finding indicates that the concentration of PPT is concentrated 1.8 times, revealing that MICM₂ can peculiarly recognize PPT from the original herb extract solution and achieve a notable enrichment effect. As a result, our study suggests a promising application of MICM₂ in the enrichment and purification of PPT from the crude extract solution of *S. emodrate*.

pH-Response of MICM₂

The effect of pH value on permeating selectivity of MICM₂ was also examined. Methacryloyl chloride or sodium methoxide was added into solutions to adjust their pH values. Sixty milliliter PPT/DMEP mixtures (200 μ g/mL of each in CH₃OH) at various pH values (2.5, 3.6, 4.6, 5.6, 7.6, 8.4, and 10.1) were used as samples in the H-shape model equipped with MICM₂, respectively. Permeating solutions at 7 h were analyzed by UPLC according to the standard curves determined using control buffer solutions. The results shown in Figure 11 indicate that the permeated amount of PPT through MICM₂ decreased with the increased pH value, while that of the competitive compound DMEP shows an increasing trend. At pH values below 8.4, MICM₂ leads to a faster transport to PPT than DMEP. The maximal permeating selectivity was achieved at pH 2.5 with a selectivity factor PPT/DMEP of 2.82. But the situation was reversed at pH values above 8.4, where MICM₂ preferentially permeated more DMEP than PPT. The observation might be attributed to the tautomerization of β -diketone ketone and enol

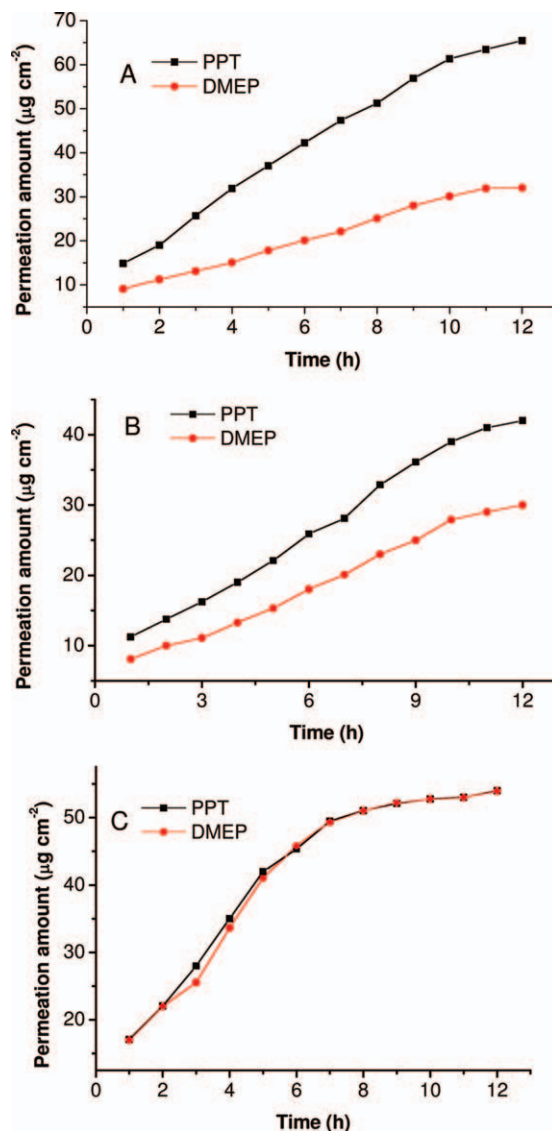


Figure 10. The permeation curves of PPT and DMEP through MICM₂ (A), NICM₂ (B), and PVDF (C). The initial solution is 60 mL PPT/DMEP CH₃OH mixture (200 μ g mL⁻¹). [Color figure can be viewed in the online issue, which is available at wileyonlinelibrary.com.]

of PMMP structure in response to the change of pH value.²⁵ This peculiar pH-controllability property would make it possible to use MICM₂ as a potential medicine control release material or separation material.

Table III. Concentration and Ratio of the Substrates in the Solution of *Sinophyllum emodrate*

Substrates	Initial extract solution	Penetration solution at 7 h	
		MICM ₂	NICM ₂
PPT (μ g mL ⁻¹)	100.6	29.46	21.09
DMEP (μ g mL ⁻¹)	5.280	0.86	1.010
PPT/DMEP ratio	19.05	34.26	20.87

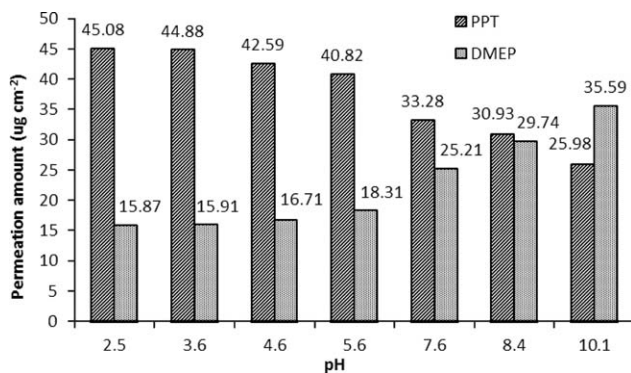


Figure 11. Permselectivity of the MICM₂ at various pH values. The initial solution is 60 mL PPT/DMEP CH₃OH mixture (200 µg mL⁻¹), the permeation time is 7 h.

CONCLUSIONS

In this study, a pH-controllable MICM₂ with "tailored" recognition sites to PPT was prepared through copolymerization of a new functional monomer PMMP and EDMA, with a PPT/PMMP/EDMA ratio of 1:4:20. The UV analysis reveals a stimuli-response of PMMP and strong complexing ability to template PPT. As a result of successful imprinting, the optimal membrane (MICM₂) showed a different porous structure and surface morphology from those of NICM₂, and can efficiently recognize PPT even in the crude extract solution of *S. emodi*. Especially, this imprinted membrane was successfully used in the competitive transport of PPT in a complex system and showed a pH-controllable effect. This peculiar property would lead this imprinted membrane to have a potential application in the separation and enrichment of PPT, and the new functional monomer PMMP exhibited an attractive application prospect in functional material fields.

ACKNOWLEDGMENTS

This work was financially supported by the Natural Science Foundation of China (No.20964005), as well as by a program for New Century Excellent Talents in University from MOE (No.NCET-08-0925), and a grant (No.2009FL03) from Yunnan Tobacco, China.

REFERENCES

- Cairnes, D. A.; Kingston, D. G.; Rao, M. M. *J. Nat. Prod.* **1981**, *44*, 34.
- Yu, P. Z.; Wang, L. P.; Chen, Z. N. *J. Nat. Prod.* **1991**, *544*, 1422.
- Ulbricht, M. *J. Chromatogr. B* **2004**, *804*, 113.
- Barahona, F.; Turiel, E.; Esteban, A. M. *Anal. Chim. Acta.* **2011**, *694*, 83.
- Vatanpoura, V.; Madaenia, S. S.; Zinadinia, S. H. R. Rajabi, J. *Membr. Sci.* **2011**, *373*, 36.
- Kochkodan, V.; Hila, N.; Melnik, V.; Kochkodand, O.; Remizovsk, A. *J. Membr. Sci.* **2011**, *377*, 151.
- Pan, G. Q.; Zhang, Y.; Guo, X. Z.; Li, C. X.; Zhang, H. Q. *Biosens. Bioelectron.* **2010**, *26*, 976.
- Cheng, C.; Ma, L.; Wu, D. F.; Ren, J.; Zhao, W. F.; Xue, J. M.; Sun, S. D.; Zhao, C. S. *J. Membr. Sci.* **2011**, *378*, 369.
- Suedee, R.; Jantararat, C.; Lindner, W.; Viernstein, H.; Songkro, S.; Srichana, T. *J. Controlled Release* **2010**, *142*, 122.
- Liang, X. Q.; Pu, X. M.; Zhou, H. W.; Wong, N. B.; Tian, A. M. *J. Mol. Struct.* **2007**, *816*, 125.
- Zhu, X. F.; Cao, Q. E.; Hou, N. B.; Ding, Z. T. *Anal. Chim. Acta* **2006**, *561*, 171.
- Remya, P. N.; Suresh, C. H.; Reddy, M. L. *Polyhedron* **2007**, *26*, 5016.
- Rolando, R. L.; Justinas, C.; Chin, W.; Chevalier, M.; Claudine, C. *Chem. Phys. Lett.* **2011**, *504*, 142.
- Wang, G. S.; Cao, Q. E.; Zhu, X. F.; Yang, X. Q.; Yang, M. H.; Ding, Z. T. *J. Appl. Polym. Sci.* **2009**, *113*, 3049.
- Songa, G.; Kellam, M. E.; Lianga, D.; Dolanb, M. D. *J. Membr. Sci.* **2010**, *363*, 309.
- Kang, S.; Xu, Y.; Zhou, L.; Pan, C. P. *J. Appl. Polym. Sci.* **2012**, *124*, 3737.
- Kusunoki, T.; Kobayashi, T. *J. Appl. Polym. Sci.* **2010**, *117*, 565.
- Wang, G. S.; Cao, Q. E.; Ding, Z. T.; Wang, Y. G.; Yang, M. H. *Helv. Chim. Acta* **2007**, *90*, 1179.
- Lawrence, E. L.; Ball, R. J.; Evans, R.; Stevens, R. *J. Power Sources* **2002**, *110*, 125.
- Qi, P. P.; Wang, J. C.; Wang, L. D.; Li, Y.; Jin, J.; Su, F.; Tian, J. *Polym.* **2010**, *51*, 5417.
- Hillberg, A. L.; Brain, K. R.; Allender, C. J. *J. Mol. Recognit.* **2009**, *22*, 223.
- Shawky, H. A. *J. Appl. Polym. Sci.* **2009**, *114*, 2608.
- Bedows, E.; Hatfield, G. M. *J. Nat. Prod.* **1982**, *45*, 725.
- Yoshimi, Y.; Arai, R.; Nakayama, S. *Anal. Chim. Acta* **2010**, *682*, 110.
- Sloop, J. C.; Bumgardner, C. L.; Washington, G.; Loehle, W. D.; Sankar, S. S.; Lewis, A. B. *J. Fluor. Chem.* **2006**, *127*, 780.